[4+2]-Cycloaddition Reactions to Corannulene Accelerated by η^6-Coordination of Ruthenium Complexes

Amir Lebcir,[a, b] Abbes Boukhari,[b] Miquel Solà,*[a] and Yago García-Rodeja*[a]

The influence of different $(LRu)_n^{II}$ (L=Cp^- (n = 1, 2); C_6H_6) moieties η^6-coordinated to corannulene (($CpRu$)$^+$, (Benzene)Ru^{2+} and ($CpRu$)$_2^{2+}$) has been explored by using the Activation Strain Model (ASM) of reactivity together with the Energy Decomposition Analysis (EDA) scheme. The results obtained have been compared with those obtained for the non-coordinated corannulene counterpart. It has been observed that the presence of the ruthenium moiety favors both kinetically and thermodynamically the [4+2]-cycloaddition reaction with cyclopentadiene. The factors governing these differences depend on the nature of the [Ru] complex. Whereas the interaction energy is solely responsible for the lower activation energy for the monocationic system ($CpRu$)$^+$, not only the higher interaction but also the lower strain energy explain the much higher reactivity observed for the dicationic systems ((C_6H_6)Ru^{2+} and ($CpRu$)$_2^{2+}$). In this latter case, the Pauli repulsion energy term is the factor controlling the differences in the interaction energies, following the so-called Pauli repulsion-lowering concept. Finally, when η^6-coordinating mono- or dicationic ruthenium complexes, although the [4+2]-cycloaddition reaction in the external *rim* bonds remains the thermodynamically and kinetically more favourable, the cycloaddition becomes also thermodynamically feasible in some internal bonds.

Introduction

Corannulene ($C_{20}H_{10}$, **1**, Figure 1a) is the smallest bowl-shaped polycyclic aromatic hydrocarbon (PAH) derived from the fullerene C_{60}. It is composed of a five-membered ring surrounded by five six-membered rings with a curved structure caused by the strain requirements of the central ring.[1] Due to its exceptional physicochemical properties, corannulene can be used in molecular electronics, energy storage, or photovoltaic materials.[2–10]

Although numerous transition metal η^2- or η^5-coordinated to fullerene C_{60} complexes have been investigated, there is less evidence of η^6-complexes.[11] Furthermore, since the synthesis of the first transition metal corannulene complexes, [$Cp^*Ru(\eta^6$-$C_{20}H_{10})$]$^+$ (**2-Me**, Figure 1b, $Cp^*=C_5Me_5$), and the dimetallated complex [$(Cp^*Ru)_2(\mu^2$-η^6,η^6-$C_{20}H_{10})$]$^{2+}$ (**4-Me**, Figure 1b) by Siegel et al. in 1997,[12] and their characterization by Angelici and coworkers in 2004,[13] and despite the potential of these type of
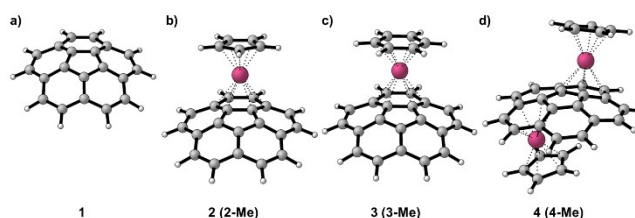
Figure 1. (a) Corannulene, **1**, and ruthenium coordinated η^6-corannulene complexes considered for this study: (b) [$CpRu(\eta^6$-$C_{20}H_{10})$]$^+$, **2**; (c) [(C_6H_6)Ru-(η^6-$C_{20}H_{10}$)]$^{2+}$, **3**; and (d) [($CpRu$)$_2(\mu^2$-η^6,η^6-$C_{20}H_{10})$]$^{2+}$, **4**, with $Cp=(C_5H_5)^-$. The counterparts with the methylated benzene and Cp ligands are denoted as **2-Me**, **3-Me**, and **4-Me**, respectively.

complexes, only a few examples of metal-complexed corannulene have been computationally or experimentally characterized.[12–25]

Moreover, as far as we know, only a reduced number of studies of the influence on the reactivity of the complexation of transition metals moieties to the corannulene have been made so far.[18]

To understand the reactivity of PAHs, the Activation Strain Model (ASM) of reactivity[26–29] and the Energy Decomposition Analysis (EDA)[30–32] were extensively used.[1,33–35] These methods were also used to investigate: (a) the influence in the [4+2]-cycloaddition reaction of replacing a CH moiety with a transition metal one,[36] (b) a C–C bond for the isoelectronic B–N bond,[37,38] and (c) a C atom for a N atom in C_{60} to form the ionic azafullerene.[39,40]

For the above reasons, we decided to apply the ASM-EDA methodology to gain deeper insight into the factors controlling the reactivity of transition metal complexes η^6-coordinated to corannulene. To this end, we explored, through density functional theory (DFT) calculations, the [4+2]-cycloaddition reac-

[a] A. Lebcir, M. Solà, Y. García-Rodeja
Institut de Química Computacional i Catàlisi and Departament de Química, Universitat de Girona, Campus Montilivi, Girona, Catalonia 17003 Spain
E-mail: miquel.sola@udg.edu
yago.garcia-rodeja@udg.edu

[b] A. Lebcir, A. Boukhari
Laboratory of Organic Synthesis, Modeling and Optimization of Chemical Processes, Department of Chemistry, Faculty of Sciences, Badji Mokhtar-Annaba University, BP 12, Annaba 23000, Algeria

EurJOC
European Journal of Organic Chemistry

Research Article
doi.org/10.1002/ejoc.202400697

Chemistry
Europe
European Chemical
Societies Publishing

tions between cyclopentadiene and corannulene complexes (Figure 1).

Computational Details

All calculations (i.e. geometry optimizations, frequency calculations, single point energy calculations) were done by using Gaussian 16 (Rev. A.03)[41] at BP86[42,43]-D3[44]/def2-TZVPP[45,46]//BP86-D3/def2-SVP level of theory. Energy Decomposition Analyses (EDA) were performed with the Amsterdam Modeling Suite (AMS version 2022.204)[47,48] at BP86-D3/TZ2P[49]//BP86-D3/def2-SVP level of theory. In the EDA,[30-32] the electronic bond energy $\triangle E$ at any point along the reaction coordinate can be decomposed into the strain energy, $\triangle E_{strain}$, associated with the deformation of the two reactants from their equilibrium structure to the geometry they adopt at a given point in the reaction coordinate plus the interaction energy, $\triangle E_{int}$, between these deformed fragments. The latter is further decomposed into the classical electrostatic attraction, $\triangle V_{elstat}$, Pauli repulsion, $\triangle E_{Pauli}$, between occupied orbitals, stabilizing orbital interactions, $\triangle E_{orb}$, and dispersion interactions, $\triangle E_{disp}$. The orbital interaction energy term is decomposed by means of the Natural Orbitals for Chemical Valence (NOCV).[50] The Multiwfn program was used for the Extended Charge Decomposition Analysis (ECDA) of the different systems.[51]

Results and Discussion

These complexes possess four different types of CC bonds where a cycloaddition reaction could take place, namely: internal *spoke* (known as [6,6], where two six-membered rings are fused) and *hub* (known as [5,6], where five- and six-membered rings are fused) bonds and external *flank* and *rim* bonds (Figure 2). Cycloaddition reactions (for instance, Prato or
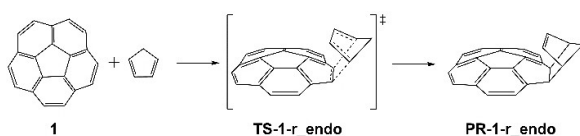
Diels-Alder) in corannulene -as in empty fullerenes- occur exclusively at the [6,6] or external bonds.[35,52]

Therefore, we decided to study the regioselectivity of the [4+2]-cycloaddition reaction of corannulene (**1**) and its ruthenium η^6-coordinated to corannulene complexes (**2–4**) with cyclopentadiene by comparing the reactivity of the four different C–C bonds (see Scheme 1 and Table 1).

To this aim and considering the similar energies and trends in the reactivities of the complexes with the ruthenium methylated or hydrogenated ligands (Table 1), we decided to carry out the study with the hydrogenated systems (depicted in Figure 1).

From the values of Table 1, we see that, in general, the methylated systems are somewhat less reactive than the hydrogenated ones, but the trends remain the same. On the other hand, the exothermicity of the reaction at both the internal (*hub* and *spoke*) and external (*rim* and *flank*) C–C bonds increases with the presence of the ruthenium moiety. It is remarkable to notice that the [6,6] and [5,6] bonds are activated when dicationic transition metal moieties are coordinated to corannulene. When η^6-coordinated mono- or dicationic ruthenium complexes are involved, the [4+2]-cycloaddition reaction on the external rim bonds remains the thermodynamically most favorable. Interestingly, the addition to some internal bonds becomes thermodynamically feasible too. A similar change in the reactivity –at the *spoke* bonds– has been observed by Fernández and co-workers when increasing the size of the system from corannulene to hemifullerene.[35]

The whole reaction profiles have been computed for the most exothermic reactions for each system (Table 2) to gain a deeper understanding of the influence of the coordination of the ruthenium moiety to corannulene on the Diels-Alder reaction of cyclopentadiene. In all cases, the most reactive bonds are those located in the rim of the corannulene molecule (**r** for **1**, **r2** for **2** and **3**, and **r1** for **4**). For **1**, **r** is any of the **r1**, **r2**, and **r3** bonds in Figure 2.

Similar to what happens with the reaction energy, the Gibbs activation energy decreases in the presence of the transition

Figure 2. Different bonds where the [4+2]-cycloaddition reaction could take place. Dark and light blue rings correspond to those rings where the [Ru] is η^6-coordinated to the convex and concave face, respectively. Where s=spoke, h=hub, f=flank, and r=rim.

Scheme 1. Schematic representation of the Diels-Alder reaction between corannulene, **1**, and cyclopentadiene in the rim, **r**, bond for the *endo* approach.

Table 1. Electronic energies in kcal mol^{-1} of the most stable (*exo* or *endo*) adducts for corannulene (**1**) and with the hydrogenated (**2–4**) or methylated (in parentheses, **2-Me**–**4-Me**) ruthenium ligands. Energy level: BP86-D3/def2-TZVPP//BP86-D3/def2-SVP (see Tables S1–S4).

Bond	1	2 (2-Me)	3 (3-Me)	4 (4-Me)
h[a]	8.7	0.8 (3.1)	−4.3 (0.6)	−5.5 (0.4)
s1[a]	10.1	0.1 (2.5)	−4.3 (0.4)	0.0 (0.2)
s2[a]	–	8.8 (9.4)	3.2 (5.7)	12.57 (15.7)
r1[b]	−11.7	−14.6 (−15.0)	−19.8 (−19.7)	−25.5 (−23.7)
r2[a]	–	−20.0 (−18.6)	−23.7 (−18.9)	−23.3 (−20.9)
r3[b]	–	–	–	−27.6 (−22.6)
f1[a]	22.4	16.6 (17.0)	7.4 (10.0)	14.9 (17.2)
f2[a]	–	22.6 (23.2)	–[c] (14.3)	17.5[b] (22.0)[b]
f3[a]	–	15.9 (16.3)	7.8 (10.3)	14.9 (16.9)

[a] *exo* isomer. [b] *endo* isomer. [c] The corresponding cycloadduct is not found on the PES.

EurJOC
European Journal of Organic Chemistry

Research Article
doi.org/10.1002/ejoc.202400697

Chemistry
Europe
European Chemical
Societies Publishing

Table 2. Computed stationary points for the most reactive bond for each corannulene complex. Electronic and Gibbs energies, the latter in parentheses, at BP86-D3/def2-TZVPP//BP86-D3/def2-SVP level of theory (see Tables S5 and S6). Energies are given in kcal mol^{-1}.

Compound	ΔE_{RC}	ΔE^{TS}	$\Delta E^{\ddagger}$	ΔE_R	ECDA[c]
1-r[a]	−4.8 (7.3)	12.5 (27.1)	17.3 (27.1)	−11.7 (6.5)	−0.112
2-r2[b]	−8.1 (4.8)	4.3 (20.2)	12.5 (20.2)	−20.0 (−0.8)	−0.236
3-r2[b]	−12.5 (0.0)	−6.0 (7.9)	6.5 (7.9)	−23.7 (−5.0)	−0.449
4-r1[b]	−10.9 (2.5)	−2.9 (12.9)	7.9 (12.9)	−27.6 (−7.6)	−0.409

[a] *endo* isomer. [b] *exo* isomer. [c] Net charge transferred from cyclopentadiene to the {Ru}-corannulene moiety (in electrons) in the transition state.

metal moiety from 27.1 kcal mol^{-1} in **1-r** to 7.9 kcal mol^{-1} in **3-r2**.

Moreover, the ECDA reveals a clear correlation between the net charge transferred –which increases drastically with the
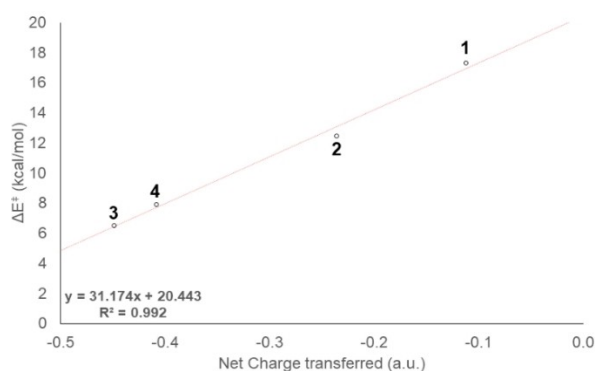
Figure 3. Linear correlation between the activation energy of the most reactive bonds for complexes **1–4** (i.e., **r**, **r2**, **r2**, and **r1**, respectively) and the net charge transferred from cyclopentadiene to the PAH moiety. Level of theory: BP86-D3/def2-TZVPP//BP86-D3/def2-SVP
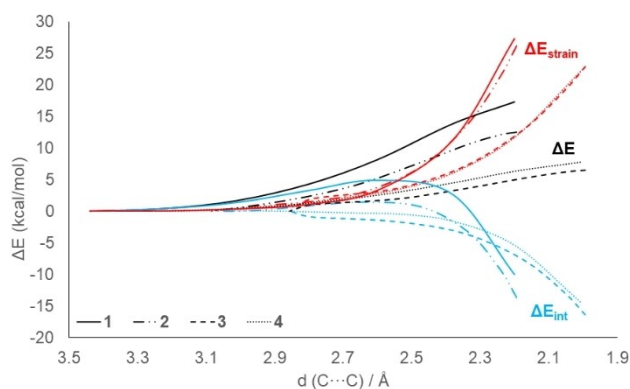
Figure 4. Activation strain diagrams for the Diels-Alder reaction between cyclopentadiene and **1** (solid lines), **2** (dash-dotted lines), **3** (dashed lines), and **4** (dotted lines) and for the most reactive bonds of each complex (see Table 2). Level of theory: BP86-D3/def2-TZVPP//BP86-D3/def2-SVP. All energies in kcal mol^{-1} are referenced to the corresponding reactant complexes.

inclusion of the transition metal– from the cyclopentadiene to the {Ru}-corannulene moiety and the activation energy of the process (Figure 3). As we will see, the higher ECDA values do not result in better interactions among frontier orbitals and the higher reactivities of the metallated complexes are caused by a Pauli repulsion lowering. We have found also a good correlation between the activation energy and the LUMO energy of complexes **1–4** (Figure S2).

Corannulene *vs.* [CpRu(η6-C20H10)]+

One may speculate that coordination with the metal reduces the available π-electrons increasing the energy barriers. However, we see that the effect is the contrary. Thus, we decided to apply the ASM-EDA methodology to discern which are the key factors controlling the reactivity of these complexes (Figure 4). In all ASM-EDA studies, we considered the reactant complex (RC) as our starting and reference point. From a geometric point of view, the neutral and monocationic systems (**1** and **2**, respectively), have earlier transition states (**TS-1-r** and **TS-2-r2**, d(C···C) ≈ 2.2 Å) than the dicationic ones **3** and **4** (**TS-3-r2** and **TS-4-r1**, d(C···C) ≈ 2.0 Å), which is unexpected from the Hammond's postulate stating that the more exothermic the reaction is, the earlier the transition state.[53] In Figure 4, the strain energy of **1** and **2** remains almost equal along the reaction coordinate, whereas the interaction energy is clearly more stabilizing for the corannulene with the [CpRu]+ moiety η6-complexed (e.g. at C···C distance of 2.3 Å, $\Delta\Delta E_{strain} \approx -2$ kcal mol^{-1} whereas $\Delta\Delta E_{int} \approx -5$ kcal mol^{-1}; $\Delta\Delta E$ values referred to **1**, i.e., $\Delta\Delta E = \Delta E_x - \Delta E_1$). When [(C6H6)Ru]$^{2+}$ or [CpRu]$_2^{2+}$ is coordinated to the corannulene not only the interaction energy plays a role in the different reactivities but also the strain energy. The inclusion of these moieties strongly decreases the strain energy required along the entire reaction (e.g. at the same C···C distance of 2.3 Å, whereas the $\Delta\Delta E_{int} \approx -5$ kcal mol^{-1}, the strain energy is less destabilizing by $\Delta\Delta E_{strain} \approx -10$ kcal mol^{-1}). However, the interaction energy (Figure 4) is more stabilizing for the dicationic systems from the reactant complex up to some point in the reaction coordinate (ca. 2.25 Å), where an inversion in the stabilities occurs.

The comparison of **1** or **2** with **3** and **4** reveals that, although the interaction energy becomes more stabilizing at a faster rate for the systems involving **1** and **2** –getting closer as the reaction evolves to the interaction energy of the dicationic complexes–, the much less destabilizing strain energy is the main responsible of the higher reactivity of the dicationic complexes compared to the neutral and monocationic ones.

The energy decomposition analysis, depicted in Figure 5, has been used to extract from the interaction energy its physically meaningful terms. This partitioning allows us to understand which are the factors governing the interaction energies for the reactions with neutral and monocationic (**1** and **2**, respectively), and on the other hand, the dicationic systems (**3** and **4**) for those pairs with the same strain energy along the reaction coordinate. Here, the Diels-Alder reaction of cyclopentadiene with corannulene complexes **1** and **2** is used to

EurJOC
European Journal of Organic Chemistry

Research Article
doi.org/10.1002/ejoc.202400697

**Chemistry
Europe**
European Chemical
Societies Publishing
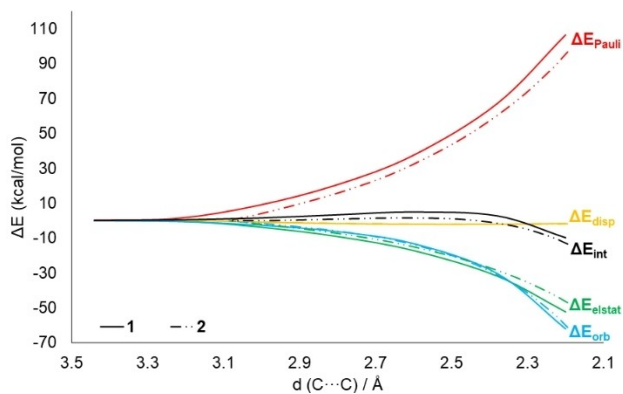
Figure 5. Energy decomposition analysis for the Diels-Alder reaction between **1** (solid lines) and **2** (dash-dotted lines) with cyclopentadiene for the most reactive bonds of each complex (see Table 2). Level of theory: BP86-D3/TZ2P//BP86-D3/def2-SVP. All energies in kcal mol^{-1} are referenced to the corresponding reactant complexes.
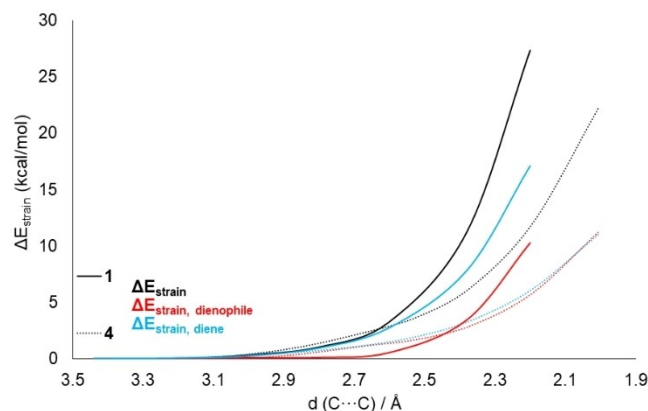
Figure 6. Decomposition of the total strain energy, ΔE_{strain}, for complex **1** and **4** into the cyclopentadiene and [Ru]$^{2+}$ moieties, ΔE_{diene} and $\Delta E_{dienophile}$, respectively. Level of theory: BP86-D3/def2-TZVPP//BP86-D3/def2-SVP. All energies in kcal mol^{-1} are referenced to the corresponding reactant complexes.

illustrate the influence of the transition metal moiety on it – compared to its non-coordinated corannulenne counterpart–.

Whereas the electrostatic interaction is more stabilizing for the reaction involving noncoordinate corannulene (**1**) along the reaction coordinate, the orbital and the dispersion ones are similar for systems **1** and **2**. The Pauli repulsion term is more favorable for **2**, explaining the lower barrier for this complex. Thus, the [CpRu]$^+$ moiety coordinated enhances the [4+2]-cycloaddition reaction with cyclopentadiene by increasing the interaction energy of the deformed reactants along the entire reaction coordinate. This effect is done by lowering the repulsive Pauli repulsion term. This reduction is driven by the charge transfer from the corannulene to the metal moiety that results in a reduction of the Pauli repulsion (because of fewer electrons in the corannulene unit) during the approximation of cyclopentadiene to corannulene.

Corannulene *vs.* [(CpRu)$_2$(μ^2-η^6,η^6-C$_{20}$H$_{10}$)]$^{2+}$

On the other hand, the presence of two [CpRu]$^+$ moieties, **4**, or the dicationic one [(C$_6$H$_6$)Ru]$^{2+}$, **3**, strongly increases the interaction energy, i.e. the reactants interact more strongly, as well as decreases the strain energy along the entire reaction coordinate (at C···C distance of 2.2 Å, $\Delta\Delta E_{int} \approx -3.7$ kcal mol^{-1} and $\Delta\Delta E_{strain} \approx -14.9$ kcal mol^{-1}, see Figures 3 and S1). The decomposition of the strain energy into their respective fragments, depicted in Figure 6, reveals that the higher strain energy for the reaction involving complex **1** is due to the higher energy required to deform both corannulene (at 2.2 Å, $\Delta\Delta E_{strain, dienophile} \approx -4.3$ kcal mol^{-1}) and cyclopentadiene moieties (at 2.2 Å, $\Delta\Delta E_{strain, diene} \approx -10.6$ kcal mol^{-1}). This means that metal complexation makes the rim bond attacked in **4** (**r-1**) geometrically more prepared for the attack of cyclopentadiene. However, the most important reduction in strain energy corresponds to cyclopentadiene. The lower Pauli repulsion experienced by cyclopentadiene approaching **4** as compared to **1** (vide infra) is translated into lower strain energy.

Moreover, the EDA analysis comparing **1** and **4** (Figure 7), in the same way as occurs comparing **1** with monocationic complex **2**, shows that whereas ΔE_{orb} and ΔE_{elstat} are more stabilizing for **1** than **4** (at 2.2 Å, $\Delta\Delta E_{orb} \approx 20.1$ kcal mol^{-1}, see Figure 8, and $\Delta\Delta E_{elstat} \approx 20.1$ kcal mol^{-1}), the Pauli repulsion energy term, ΔE_{Pauli}, is much less destabilizing for the dicationic complex (at 2.2 Å, $\Delta\Delta E_{Pauli} \approx -43.2$ kcal mol^{-1}), compensating the lower stabilizing energy terms. The decomposition of the orbital interaction in their NOCV terms shows that the higher orbital stabilization for **1** is mainly due to a more stabilizing HOMO$_{dienophile}$→LUMO$_{diene}$ interaction ($\Delta\Delta E(\rho 2) = -14.63$ kcal mol^{-1} whereas the $\Delta\Delta E(\rho 1) = -4.52$ kcal/mol). In reactions where the Pauli repulsion energy term is the key factor governing the activation energy of the process was recently named by Hamlin and co-workers as the "Pauli repulsion-lowering" effect.[54]

Thus, the much higher reactivity of the dicationic systems is related to the reduced Pauli repulsion energy term driven by
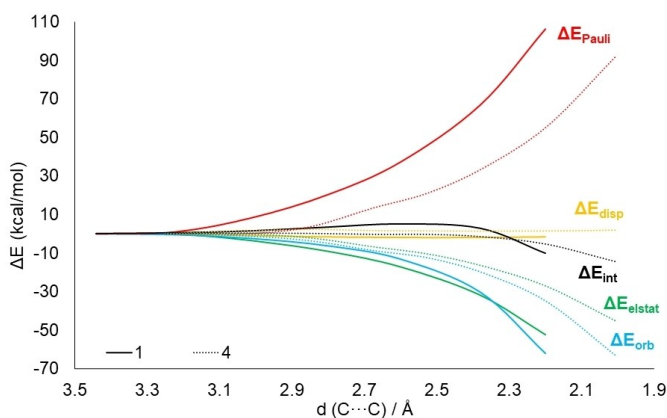
Figure 7. Energy decomposition analysis for the Diels-Alder reaction between **1** (solid lines) and **4** (dotted lines) with cyclopentadiene for the most reactive bonds (see Table 2). Level of theory: BP86-D3/TZ2P//BP86-D3/def2-SVP. All energies in kcal mol^{-1} are referenced to the corresponding reactant complexes.

EurJOC
European Journal of Organic Chemistry

Research Article
doi.org/10.1002/ejoc.202400697

Chemistry
Europe
European Chemical
Societies Publishing
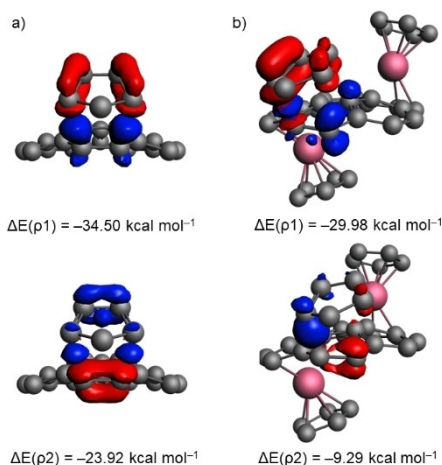
Figure 8. Plot of the deformation densities $\Delta\rho$ of the pairwise orbital interactions between cyclopentadiene and the PAH fragment (top HOMO$_{diene}$-LUMO$_{dienophile}$ and bottom HOMO$_{dienophile}$-LUMO$_{diene}$) a) corannulene, **1**, and b) [(CpRu)$_2$(μ^2-η^6,η^6-C$_{20}$H$_{10}$)]$^{2+}$, **4** and their associated stabilization energies ΔE in kcal mol^{-1}. The color code of the charge flow is red→blue.

the charge transfer for corannulene to {Ru} moieties as well as the less destabilizing strain energy of both fragments and not due to more stabilizing orbital or electrostatic interactions.

Conclusions

This study reflects the main factors governing the different [4+2]-cycloaddition reactivities of cyclopentadiene with ruthenium coordinated, i.e. CpRu$^+$, (C$_6$H$_6$)Ru^{2+}, and (CpRu)$_2^{2+}$, η^6-corannulene complexes, **2–4**, compared with the non-coordinated corannulene analog, **1**. It has been observed that both internal and external C–C bonds become more reactive when a ruthenium complex is coordinated with corannulene. Moreover, in the dicationic systems **3** and **4**, the internal [5,6] and [6,6] bonds are activated by the presence of the transition metal moiety. On one hand, when focusing on the influence of the inclusion of one CpRu$^+$ moiety, i.e. comparing **1** and **2**, the results obtained showed that the sole factor increasing the reactivity of the metallated systems is the interaction energy, ΔE_{int}, between both fragments. This higher interaction energy term is due to a lower Pauli repulsion term.

On the other hand, when comparing the neutral system **1** with the dicationic one **4**, it has been observed that the much higher reactivity of **4** ($\Delta\Delta E^\ddagger = -9.4$ kcal mol^{-1}) is now because of both, a less destabilizing strain energy along the entire reaction coordinate as well as a more stabilizing interaction energy. The decomposition of the strain energy reveals that complex **4** required much less energy to deform both reactants, particularly the diene, during the entire reaction. The energy decomposition analysis reveals the Pauli repulsion term is the main factor contributing to the lower interaction energy computed for the dimetallated system **4**. Both scenarios agree with the so-called Pauli repulsion-lowering concept developed by Hamlin and co-workers. In addition, the charge analysis

carried out by using ECDA reveals that increasing the charge donation from cyclopentadiene to the PAH moiety strongly enhances the Diels-Alder reaction. Therefore, it can be concluded that the inclusion of a transition metal moiety, as well as the nature of its ligand, are key aspects of the improved Diels-Alder reactivity of η^6-corannulene complexes. This study shows a new way to functionalize corannulene complexes, activating internal and external C–C bonds by η^6-coordinating ruthenium complexes.

Supporting Information Summary

Supporting Information contains Tables with electronic and Gibbs reaction energies and reaction barriers for the most and least stable isomers (*endo* and *exo*). Cartesian coordinates (in Å) with ZPE corrected electronic and Gibbs energies (in a.u.) for all optimized species.

Conflict of Interests

The authors declare no conflict of interest.

Data Availability Statement

The data that support the findings of this study are available in the supplementary material of this article.

Keywords: Corannulene · Transition metal · Cycloaddition · Activation strain model · Energy decomposition analysis

[1] I. Fernández, *Chem. Sci.* **2020**, *11*, 3769.
[2] E. Nestoros, M. C. Stuparu, *Chem. Commun.* **2018**, *54*, 6503.
[3] M. Parschau, R. Fasel, K. H. Ernst, O. Gröning, L. Brandenberger, R. Schillinger, T. Greber, A. P. Seitsonen, Y. T. Wu, J. S. Siegel, *Angew. Chem. Int. Ed.* **2007**, *46*, 8258.
[4] L. Zoppi, L. Martin-Samos, K. K. Baldridge, *J. Am. Chem. Soc.* **2011**, *133*, 14002.
[5] J. Mack, P. Vogel, D. Jones, N. Kaval, A. Sutton, *Org. Biomol. Chem.* **2007**, *5*, 2448.
[6] B. M. Schmidt, D. Lentz, *Chem. Lett.* **2014**, *43*, 171.
[7] Y. T. Wu, D. Bandera, R. Maag, A. Linden, K. K. Baldridge, J. S. Siegel, *J. Am. Chem. Soc.* **2008**, *130*, 10729.
[8] L. T. Scott, P. C. Cheng, M. M. Hashemi, M. S. Bratcher, D. T. Meyer, H. B. Warren, *J. Am. Chem. Soc.* **1997**, *119*, 10963.
[9] Y. L. Wu, M. C. Stuparu, C. Boudon, J. P. Gisselbrecht, W. B. Schweizer, K. K. Baldridge, J. S. Siegel, F. Diederich, *J. Org. Chem.* **2012**, *77*, 11014.

[10] G. Valenti, C. Bruno, S. Rapino, A. Fiorani, E. A. Jackson, L. T. Scott, F. Paolucci, M. Marcaccio, *J. Phys. Chem. C* **2010**, *114*, 19467.

[11] A. Hirsch, M. Brettreich, *Fullerenes*, Wiley, Weinheim, **2004**.

[12] T. J. Seiders, K. K. Baldridge, J. M. O'Connor, J. S. Siegel, *J. Am. Chem. Soc.* **1997**, *119*, 4781.

[13] P. A. Vecchi, C. M. Alvarez, A. Ellern, R. J. Angelici, A. Sygula, R. Sygula, P. W. Rabideau, *Angew. Chem. Int. Ed.* **2004**, *43*, 4497.

[14] C. M. Alvarez, R. J. Angelici, A. Sygula, R. Sygula, P. W. Rabideau, *Organometallics* **2003**, *22*, 624.

[15] A. S. Filatov, A. Yu. Rogachev, E. A. Jackson, L. T. Scott, M. A. Petrukhina, *Organometallics* **2010**, *29*, 1231.

[16] S. N. Spisak, J. Li, A. Yu. Rogachev, Z. Wei, T. Amaya, T. Hirao, M. A. Petrukhina, *Organometallics* **2017**, *36*, 4961.

[17] J. R. Green, R. C. Dunbar, *J. Phys. Chem. A* **2011**, *115*, 4968.

[18] D. Caraiman, G. K. Koyanagi, L. T. Scott, D. V. Preda, D. K. Bohme, *J. Am. Chem. Soc.* **2001**, *123*, 8573.

[19] T. Amaya, Y. Takahashi, T. Moriuchi, T. Hirao, *J. Am. Chem. Soc.* **2014**, *136*, 12794.

[20] R. C. Dunbar, *J. Phys. Chem. A* **2002**, *106*, 9809.

[21] S. H. Martínez, S. Pan, J. L. Cabellos, E. Dzib, M. A. Fernández-Herrera, G. Merino, *Organometallics* **2017**, *36*, 2036.

[22] . W. Stoddart, J. H. Brownie, M. C. Baird, H. L. Schmider, *J. Organomet. Chem.* **2005**, *690*, 3440.

[23] J. S. Siegel, K. K. Baldridge, A. Linden, R. Dorta, *J. Am. Chem. Soc.* **2006**, *128*, 10644.

[24] B. Zhu, A. Ellern, A. Sygula, R. Sygula, R. J. Angelici, *Organometallics* **2007**, *26*, 1721.

[25] P. A. Vecchi, C. M. Alvarez, A. Ellern, R. J. Angelici, A. Sygula, R. Sygula, P. W. Rabideau, *Organometallics* **2005**, *24*, 4543.

[26] P. Vermeeren, S. C. C. van der Lubbe, C. Fonseca Guerra, F. M. Bickelhaupt, T. A. Hamlin, *Nat. Protoc.* **2020**, *15*, 649.

[27] P. Vermeeren, T. A. Hamlin, F. M. Bickelhaupt, *Chem. Commun.* **2021**, *57*, 5880.

[28] F. M. Bickelhaupt, K. N. Houk, *Angew. Chem. Int. Ed.* **2017**, *56*, 10070.

[29] I. Fernández, F. M. Bickelhaupt, *Chem. Soc. Rev.* **2014**, *43*, 4953.

[30] I. Fernández, "Energy Decomposition Analysis and Related Methods" in *Applied Theoretical Organic Chemistry*, D. J. Tantillo, Ed., World Scientific Publishing, New Jersey, **2018**, 191–226.

[31] M. von Hopffgarten, G. Frenking, *WIREs Comput. Mol. Sci.* **2012**, *2*, 43.

[32] F. M. Bickelhaupt, E. J. Baerends, *Rev. Comput. Chem.* **2000**, *15*, 1.

[33] S. Osuna, K. N. Houk, *Chem. Eur. J.* **2009**, *15*, 13219.

[34] Y. García-Rodeja, M. Solà, I. Fernández, *J. Org. Chem.* **2018**, *83*, 3285.

[35] Y. García-Rodeja, M. Solà, F. M. Bickelhaupt, I. Fernández, *Chem. Eur. J.* **2016**, *22*, 1368.

[36] Y. García-Rodeja, I. Fernández, *Chem. Eur. J.* **2017**, *23*, 6634.

[37] Y. García-Rodeja, I. Fernández, *J. Org. Chem.* **2016**, *81*, 6554.

[38] Y. García-Rodeja, I. Fernández, *Chem. Eur. J.* **2019**, *25*, 9771.

[39] Y. García-Rodeja, M. Solà, I. Fernández, *J. Org. Chem.* **2017**, *82*, 754.

[40] Y. García-Rodeja, M. Solà, I. Fernández, *Phys. Chem. Chem. Phys.* **2018**, *20*, 28011.

[41] Gaussian 16, Revision A.03, M. J. Frisch, G. W. Trucks, H. B. Schlegel, G. E. Scuseria, M. A. Robb, J. R. Cheeseman, G. Scalmani, V. Barone, G. A. Petersson, H. Nakatsuji, X. Li, M. Caricato, A. V. Marenich, J. Bloino, B. G. Janesko, R. Gomperts, B. Mennucci, H. P. Hratchian, J. V. Ortiz, A. F. Izmaylov, J. L. Sonnenberg, D. Williams-Young, F. Ding, F. Lipparini, F. Egidi, J. Goings, B. Peng, A. Petrone, T. Henderson, D. Ranasinghe, V. G. Zakrzewski, J. Gao, N. Rega, G. Zheng, W. Liang, M. Hada, M. Ehara, K. Toyota, R. Fukuda, J. Hasegawa, M. Ishida, T. Nakajima, Y. Honda, O. Kitao, H. Nakai, T. Vreven, K. Throssell, J. A. Montgomery, Jr., J. E. Peralta, F. Ogliaro, M. J. Bearpark, J. J. Heyd, E. N. Brothers, K. N. Kudin, V. N. Staroverov, T. A. Keith, R. Kobayashi, J. Normand, K. Raghavachari, A. P. Rendell, J. C. Burant, S. S. Iyengar, J. Tomasi, M. Cossi, J. M. Millam, M. Klene, C. Adamo, R. Cammi, J. W. Ochterski, R. L. Martin, K. Morokuma, O. Farkas, J. B. Foresman, D. J. Fox, Gaussian, Inc., Wallingford CT, **2016**.

[42] J. P. Perdew, *Phys. Rev. B* **1986**, *33*, 8822.

[43] A. D. Becke, *Phys. Rev. A* **1988**, *38*, 3098.

[44] S. Grimme, J. Antony, S. Ehrlich, H. Krieg, *J. Chem. Phys.* **2010**, *132*, 154104.

[45] F. Weigend, *Phys. Chem. Chem. Phys.* **2006**, *8*, 1057.

[46] F. Weigend, R. Ahlrichs, *Phys. Chem. Chem. Phys.* **2005**, *7*, 3297.

[47] E. J. Baerends et al. ADF 2022, SCM, Theoretical Chemistry, Vrije Universiteit, Amsterdam, The Netherlands, http://www.scm.com.

[48] G. te Velde, F. M. Bickelhaupt, E. J. Baerends, C. Fonseca Guerra, S. J. A. van Gisbergen, J. G. Snijders, T. Ziegler, *J. Comput. Chem.* **2001**, *22*, 931.

[49] J. G. Snijders, P. Vernooijs, E. J. Baerends, *At. Data Nucl. Data Tables* **1981**, *26*, 483.

[50] M. Mitoraj, A. Michalak, *J. Mol. Model.* **2007**, *13*, 347.

[51] T. Lu, F. Chen, *J. Comput. Chem.* **2012**, *33*, 580.

[52] I. Fernández, M. Solà, F. M. Bickelhaupt, *Chem. Eur. J.* **2013**, *19*, 7416.

[53] G. S. Hammond, *J. Am. Chem. Soc.* **1955**, *77*, 334.

[54] T. A. Hamlin, F. M. Bickelhaupt, I. Fernández, *Acc. Chem. Res.* **2021**, *54*, 1972.